The Journal of the Oceanological Society of Korea
Vol. 20, No. 1, p.56~73, April 1985.

Observed and Computed Tidal Currents in the East China Sea

Byung-Ho Choi
Dept. of Civil Engineering, Sungkyunkwan University, Suwon 170

東支那海의 觀測潮流 및 計算潮流

崔 秉 昊
成均館大學 土木工學科

Abstract: The three-dimensional hydrodynamic numerical model of the Yellow Sea and the East China Sea has been further utilised to provide S_2, K_1, O_1 tidal currents distribution in addition to previously provided M_2 tidal current distribution (Choi, 1984), especially the vertical variation of horizontal current in the region. Model results have been compared with current meter data acquired from recent China-USA Marine Sedimentation Dyamics Programme (Larsen and Cannon, 1983). Results were also used to provide maps of the S_2, K_1, O_1 tidal current constants and tidal ellipses at three depths to complement previous M_2 tidal current information.

要約: 黃海 및 東支那海의 三次元 水動力學的 數値모델이 前報告된 主太陰半日週潮(M_2)의 潮流分布(崔, 1984)에 附加하여 S_2, K_1 및 O_1 分潮의 水深에 따른 潮流分布를 算定하는 데 利用되었다. 모델結果는 近年의 美·中共 共同海洋觀測프로그램의 潮流觀測値(Larsem과 Cannon, 1983)와 比較檢討되었으며 또한 S_2, K_1 및 O_1 分潮의 表層, 中間水深, 海底에서의 潮流 調和常數 分布圖 및 潮流楕圓圖로서 提示되었다.

INTRODUCTION

The three-dimensional hydrodynamic numerical model has a grid resolution of 1/5° latitude by 1/4° longitude and covers the entire Yellow Sea and the East China Sea continental shelf. This is the same grid system as that used in the two-dimensional shelf model of Choi (1980). The hydrodynamic equations used in the model are linear with the exception of a quadratic bottom friction. Solutions are obtained by Galerkin method with an expansion of currents through the vertical water colum in terms of simple cosine functions.

The numerical techniques are based on modelling efforts at the Bidston Observatory (Heaps, 1972; Davies, 1980). The developed three-dimensional model of the East China Sea was previously utilised to reproduce the three-dimensional current structure of the M_2 tide representing the dominant tidal condition of the region (Choi, 1984). In the present study the major Constituents of the tides S_2, K_1, O_1 including the dominant tidal constituent M_2 were investigated from the extended model run. Tidal constants of M_2, S_2, K_1, O_1 tides deuced from the shelf edge of existing charts (Ogura, 1933) and a limited number of analyses of coastal and island tidal records are introduced along the open boundaries of the medel. The mean values used for deuction of individual constants were $H_{S_2}/H_{M_2}=0.4$, $K_{S_2}-K_{M_2}=35°$, and $H_{O_1}/H_{K_1}=0.7$, $K_{K_1}-K_{O_1}=20°$. The model was run for 17 days and harmonic analyses for each of the model elements were performed over 15 days of hourly data after discarding

Manuscript received 20 October 1984.

the first two days of data to allow the damping out of transients.

The computed results were compared with current measurements from USA-China Marine Sedimentation Dynamics Study (Larsen and Cannon, 1983). Reasonable agreement was found between the observations and model results, thus supporting the computed distribution of the tidal currents in the region.

NUMERICAL MODEL

The equations of continuity and motion for homogeneous water neglecting non-linear terms. shear in the horizontal and the direct influence of the tide-generating potentials, may be written in spherical polar coordinates as

$$\frac{\partial \xi}{\partial t}+\frac{1}{R\cos\phi}\left\{\frac{\partial}{\partial \chi}\int_0^h u\,dz+\frac{\partial}{\partial \phi}\int_0^h v\cos\phi\,dz\right\}=0, \tag{1}$$

$$\frac{\partial u}{\partial t}-\gamma v=\frac{-g}{R\cos\phi}\frac{\partial \xi}{\partial \chi}+\frac{\partial}{\partial z}\left(N\frac{\partial u}{\partial z}\right), \tag{2}$$

$$\frac{\partial v}{\partial t}+\gamma u=\frac{-g}{R}\frac{\partial \xi}{\partial \phi}+\frac{\partial}{\partial z}\left(N\frac{\partial v}{\partial z}\right), \tag{3}$$

were

- χ, ϕ east-longitude and north-latitude, respectively
- z depth below the undisturbed surface
- t time
- ξ elevation of the sea surface above the undisturbed level
- h undisturbed depth of water
- ρ the density of sea water
- R the radius of the Earth
- γ Coriolis parameter ($\gamma=2\omega\sin\phi$)
- ω angular speed of the Earth's rotation
- g the acceleration due to gavity
- u, v the east-going and north-going components of current at depth z
- N coefficient of vertial eddy viscosity.

In order to solve Eqs. (1), (2) and (3) for ξ, u and v, the appropriate boundary conditions at the sea surface and sea bed have to be specified.

For tides, the surface condition is

$$-\rho\left(N\frac{\partial u}{\partial z}\right)_0=-\rho\left(N\frac{\partial v}{\partial z}\right)_0=0, \tag{4a, b}$$

with the subscript zero denoting at $z=0$. Assuming a slip boundary condition at the sea bed ($z=h$) and using a quadratic law of bottom friction yields,

$$-\rho\left(N\frac{\partial u}{\partial z}\right)_h=K\rho u_h(u_h^2+v_h^2)^{1/2}, \tag{5a}$$

$$-\rho\left(N\frac{\partial v}{\partial z}\right)_h=K\rho v_h(u_h^2+v_h^2)^{1/2}, \tag{5b}$$

where K is the coefficient of quadratic bottom friction, taken as constant.

Expanding the two comoponents of velocity u, v in terms of m depth-dependent functions $f_r(z)$ (the basis functions), and the horizontal-space and time dependent coefficients $A_r(\chi, \phi, t)$ and $B_r(\chi, \phi, t)$ gives:

$$u(\chi, \phi, z, t)=\sum_{r=1}^{m} A_r(\chi, \phi, t)\, f_r(z), \tag{6}$$

$$v(\chi, \phi, z, t)=\sum_{r=1}^{m} B_r(\chi, \phi, t)\, f_r(z). \tag{7}$$

Using the Galerkin method in the vertical space domain, Eqs. (2) and (3) are multiplied by each basis functions f_k and integrated over the region 0 to h with respect to z. By integrating the term involving the vertical eddy viscosity, boundary conditions (4a, b) and (5a, b) can be incorporated, giving

$$\int_0^h \frac{\partial u}{\partial t}f_k dz=\gamma\int_0^h v f_k dz-\frac{g}{R\cos\phi}\frac{\partial \xi}{\partial \chi}\int_0^h f_k dz-f_k(h)Ku_h(u_h^2+v_h^2)^{1/2}-\int_0^h N\frac{\partial u}{\partial z}\frac{\partial f_k}{\partial z}dz, \tag{8}$$

$$\int_0^h \frac{\partial v}{\partial t}f_k dz=-\gamma\int_0^h u f_k dz-\frac{g}{R}\frac{\partial \xi}{\partial \phi}\int_0^h f_k dz-f_k(h)Kv_h(u_h^2+v_h^2)^{1/2}-\int_0^h N\frac{\partial v}{\partial z}\frac{\partial f_k}{\partial z}dz, \tag{9}$$

where $k=1,2,\cdots,m$. From Eqs. (8) and (9) the bottom boundary conditions occur in these equations as products with $f_k(h)$ and therefore if this product is to nonzero, the f_k must be chosen such that

$$f_k(h) \neq 0 \tag{10}$$

for $k=1,2,\cdots,m$.

For the choice of basis functions $f_r(z)$, Davies (1980) has show that an expansion of only 10 cosine functions is sufficient to accurately reproduce the depth variation of current and has applied such an expansion to the computation of the M_2 tide of the North-West European Continental Shelf.

In the present study adopting the expansion of 10 cosine functions with f_r given by

$$f_r=\cos\ \alpha_r \frac{z}{h} \tag{11}$$

and a suitable choice α_r is

$$\alpha_r=(r-1)\pi, \quad r=1,2,\cdots,m. \tag{12}$$

in which case

$$f_r'(0)=0, \tag{13}$$

and

$$f_r'(h)=0, \tag{14}$$

where

$$f_r'=df_r/dz.$$

The particular case in which the vertical eddy viscosity N is independent of depth coordinate z is considered. The f_r given by Eq. (11) are eigenfunctions of

$$\frac{d}{dz}\{N(\chi,\phi,t)\ f_r'(z)\}=-\lambda(\chi,\phi,t)\ f_r(z) \tag{15}$$

with eigenvalues $\lambda_r(\chi,\phi,t)$ given by

$$\lambda_r(\chi,\phi,t)=N(\chi,\phi,t)\ \alpha_r^2/h^2. \tag{16}$$

Integrating by parts the terms involving N in (8) and (9), using (15), (16), (13) and (14) and substituting expansions (6) and (7) into (8) and (9) gines a set of partial differential equations involving ξ, Ar and Br. Details of the formulation were given by Davies (1980) and will not be restated here. These equations can then be integrated forward through time to find the variation of ξ, Ar and Br over the modelled sea area, subject to initial and boundary conditions. Currents at any depth can be calculated from the Ar and Br using expansions (6) and (7). In order to solve the equations it is necessary to discretize in the horizontal and with time. Discretization in the horizontal is accomplished by using a staggered finite-difference grid, in which ξ, u and v are evaluated at different grid points. Solutions are generated from a state of rest, expressed by

$$\xi=Ar=Br=0 \text{ at } t=0, \ (r=1,2,\cdots,m) \tag{17}$$

Along a closed boundary the normal component of current is set to zero. for all $t\geqslant 0$, thus

$$Ar\ \cos\ \phi+Br\ \sin\ \phi=0, \ (r=1,2,\cdots,m), \tag{18}$$

where ϕ denotes the inclination of the normal to the direction of increasing χ.

Along the open boundaries of the model, M_2, S_2, K_1 and O_1 tidal input determined from the two-dimensional model (Choi, 1980) is specified and a radiation condition is employed to allow disturbances from the interior of the model to pass outward. This condition involves a prescribed relation between the total normal component of depth-mean current q and total elevation ξ given by:

$$q=q_T+\frac{c}{h}(\xi-\xi_T) \tag{19}$$

where $c=(gh)^{1/2}$. The change in sea surface elevation ξ_T, arising from the i^{th} tide denoting M_2, S_2, K_1 and O_1 tides is given by:

$$\xi_T=H_i\ \cos\ \{\sigma_i t-\kappa_i\} \tag{20}$$

and

$$q_T=Q_i\ \cos\ \{\sigma_i\ t-\gamma_i\}. \tag{21}$$

In Eqs. (20) and (21) H_i and Q_i denote the amplitude of $_ith$ tidal elevation and the amplitude of the normal component of depth-mean $_ith$ tidal current respectively. Also, κ_i and γ_i denote the phase of $_ith$ tidal eveation and the phase of the normal component of depth-mean $_ith$ tidal current. These values were derived pre-

viously in computing the distribution of the M_2, S_2, K_1 and O_1 tides in the East China Sea Continental Shelf with a two-dimensional model. Using Eq. (19) with ξ_T and q_T determined from (20) and (21), the depth-mean current around the edge of the continental shelf may be computed. However Eq. (19) gives no information on the contribution of the various terms in the expansions to the depth-mean current. It is necessary to make an assumption about the contribution of each term in expansions (6) and (7) to this depth-mean current. The assumption made was that only the first term in each expansion contributed to the current at the continental shelf edge. Thus A^1 and B_1 are given by

$$A_1 = \frac{q_u}{a_1}, \quad B_1 = \frac{q_v}{a_1}\left(a_1 = \frac{1}{h}\int_0^h f_1(Z)dz\right) \tag{22}$$

and

$$Ar = Br = 0, \quad (r = 2, 3, \cdots, m). \tag{23}$$

where q_u and q_v are respectively the u and v components of depth-mean current given by (19). Heaps (1972) has shown that above assumption does not severely affect the computed current profiles within the three-dimensional region.

MODEL RESULTS

Eight current measurements in the modelled region came from current meter positioned in Fig. 1. As shown the current meter rigs were mainly concentrated across the continental shelf edge along approximately 32°N. A detailed description of results from the measurements is given by Larsen and Cannon (1983).

In order to make comparison between computed and observed currents, it is necessary to compare amplitudes and phases of the u component (easterly component) and x component (northerly component) of current. Computed and observed values of amplitude H (cm/sec.) and phase K (degree referred to 135°E) for u

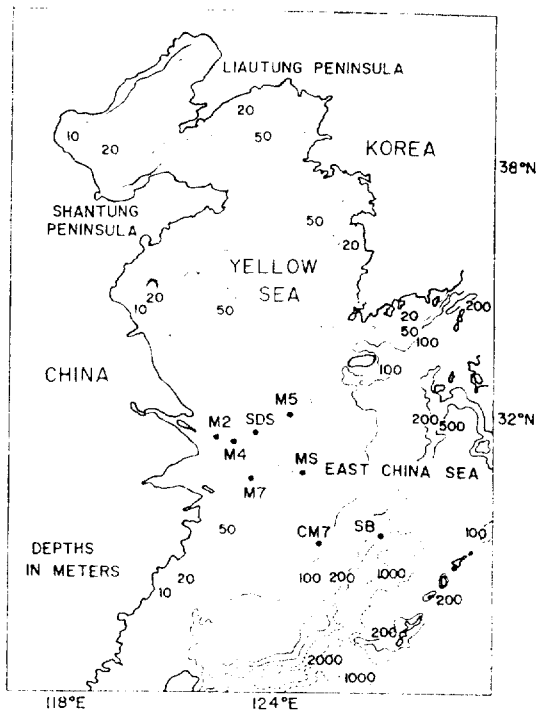

Fig. 1. Position of current meter rig.

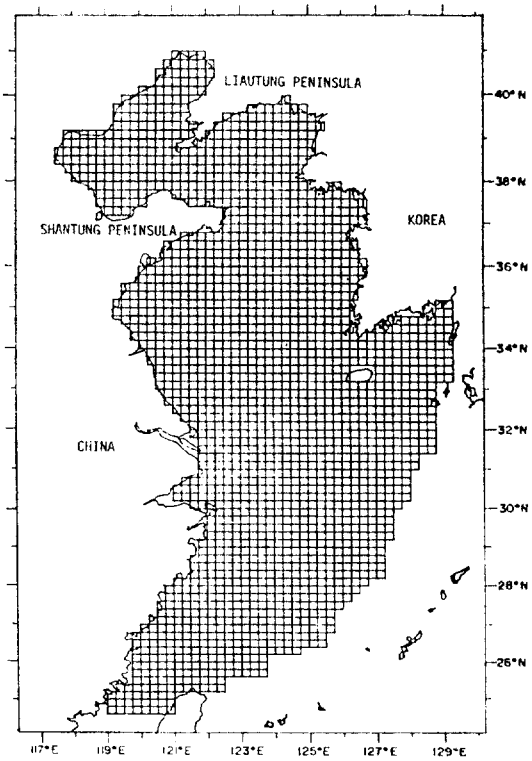

Fig. 2. Finite-difference grid of three-dimensional model.

Table 1. Comparison of observed and computed amplitudes (cm/sec.) and phase k (degree referred to 135°E) for u and v component of S_2 tidal current.

Current meter rig	Position (Latitude Longitude)	Observed u H	Observed u k	Observed v H	Observed v k	depth	Calculated u H	Calculated u k	Calculated v H	Calculated v k	depth
M2	31.40 N 122.37 E	33	176	33	60	4	33	176	26	69	surface
M4	31.25 N 122.82 E	17 11	119 143	21 22	359 360	2 44	26 14	173 167	17 8	53 45	surface bottom
M5	32.00 N 124.50 E	17	144	18	40	20	25	150	20	53	mid-depth
M7	30.33 N 123.44 E	14 7	111 143	17 10	14 18	5 60	13 7	164 160	14 7	12 355	surface bottom
SB	28.91 N 127.25 E	5	38	4	247	177	5	77	2	291	bottom
MS	30.52 N 124.80 E	12 9	85 66	10 9	342 329	23 45	17 10	132 127	11 6	4 3	mid-depth bottom
SDS	31.46 N 123.50 E	6	61	10	331	bottom	13	159	10	55	bottom
CM7	28.65 N 125.45 E	16	72	10	307	20	8	92	7	310	mid-depth

Table 2. Comparison of observed and computed amplitudes (cm/sec.) and phase k (degree referred to 135°E) for u and v component of K_1 tidal current.

Current meter rig	Position (Latitude Longitude)	Observed u H	Observed u k	Observed v H	Observed v k	depth	Calculated u H	Calculated u k	Calculated v H	Calculated v k	depth
M2	31.40 N 122.37 E	10	348	10	298	4	6	328	9	279	surface
M4	31.25 N 122.82 E	3 5	314 242	11 9	301 342	2 44	5 2	335 333	7 4	294 292	surface bottom
M5	32.00 N 124.50 E	5	69	8	324	20	9	354	11	260	mid-depth
M7	30.33 N 123.44 E	21 2	336 297	17 3	261 38	5 60	3 2	343 340	2 1	247 252	surface bottom
SB	28.91 N 127.25 E	1	238	2	155	177	1	26	1	229	bottom
MS	30.52 N 124.80 E	6 3	339 322	8 4	270 315	23 45	4 3	348 348	5 2	242 241	mid-depth bottom
SDS	31.46 N 23.50 E	3	213	3	350	bottom	3	350	5	274	bottom
CM7	28.65 N 125.45 E	3	270	2	140	20	2	237	2	146	mid-depth

and v at eight current meter rigs are given in Tables 1-3. It is seen from the tables that general agreement between the observations and model results has been demonstrated. It is worth mentioning that positional discrepancy between the current observation points and nearby model calculation points could be in error by as much as 0.2 degrees. Initial calculations were made at three representative depths in the present study although the model could compute a continuous current profile with depth. Spatial distribution of coamplitude and cophase lines for u and v components of S_2, K_1, O_1 tidal currents at sea surface, mid-depth and sea bed are shown in Fig. 3. ~Fig. 8. It is seen from the figures of cophase lines that there are nodal

Table 3. Comparison of observed and computed amplitudes (cm/sec.) and phase k (degree referred to 135°E) for u and v component of O_1 tidal current.

Current mater rig	Position (Latitude Longitude)	Observed				depth	Calculated				depth
		u		v			u		v		
		H	k	H	k		H	k	H	k	
M2	31.40 N 122.37 E	11	291	10	260	4	4	279	8	228	surface
M4	31.25 N	4	212	9	266	2	3	281	7	250	surface
	122.82 E	5	169	4	265	44	2	293	4	246	bottom
M5	32.00 N 124.50 E	5	17	8	277	20	8	314	10	218	mid-depth
M7	30.33 N	15	284	9	215	5	2	298	2	242	surface
	123.44 E	1	155	3	340	60	1	292	1	243	bottom
SB	28.91 N 127.25 E	1	270	1	235	177	1	340	1	244	bottom
MS	30.52 N	4	340	6	250	23	3	330	3	231	mid-depth
	124.80 E	3	345	4	268	45	2	331	2	231	bottom
SDS	31.46 N 123.50 E	3	218	3	263	bottom	2	314	4	233	bottom
CM7	28.65 N 125.45 E	1	140	2	12	20	2	131	2	43	mid-depth

points on the shelf, where either the u or v component current is zero. Significant phase change through depth may occur in the vicinity of these nodal points because the position of these nodes varies from sea surface to sea bed.

For S_2 tidal current, amplitude difference of 20～30cm/sec. for u component and 10cm/sec. for v component between sea surface and bottom occur in Hangzhou Bay, Inchon Bay and Seohan Bay. Phase difference of about 30° for u component and 10°～20° for v component between sea surface and bottom occur throughout the modelled region except a u nodal point at the shelf.

For K_1 tidal current, amplitude difference of 10～15cm/sec. for u component and 5～10cm/sec. for v component between sea surface and bottom occur in the southern part of Liautung Gulf and seas adjacent to the east of Jeju Island. Phase difference of 10°～20° for u component and 5°～10° for v component between sea surface and bottom throughout the shelf. Large phase difference occur near the u nodal points in the offshore of mid-Chinese coast, offshore of southwestern tip of Korea, southern part of Hangzhou Bay and several u nodal points along the shelf edge. Large phase difference also occur v nodal point near the Pohai Strait.

For O_1 tidal current, amplitude difference of 10cm/sec. for u component and 5～10cm/sec. for v component between sea surface and bottom occur at the Pohai Strait and shelf edge near Kyushu Islands. Phase difference of 10°～15° for u component and 5°～10° for v component between sea surface and bottom occur throughout the shelf. Large phase difference for u comonent occur near offshore of mid-Chinese coast and offshore of southwestern tip of Korea. Significant phase difference of both u and v component of O_1 tidal current occur in the central region of East China Sea shelf.

Magnitudes and directions of the principal axes of the S_2, K_1, O_1 tidal current ellipses at the sea surface, mid-depth and sea bed are given in Fig. 9～Fig. 11. The sense of rotation of the current vector is shown by the very small tick mark at the end of a line which indicates the position of current vector at the time of lunar transit at 135° east longitude.

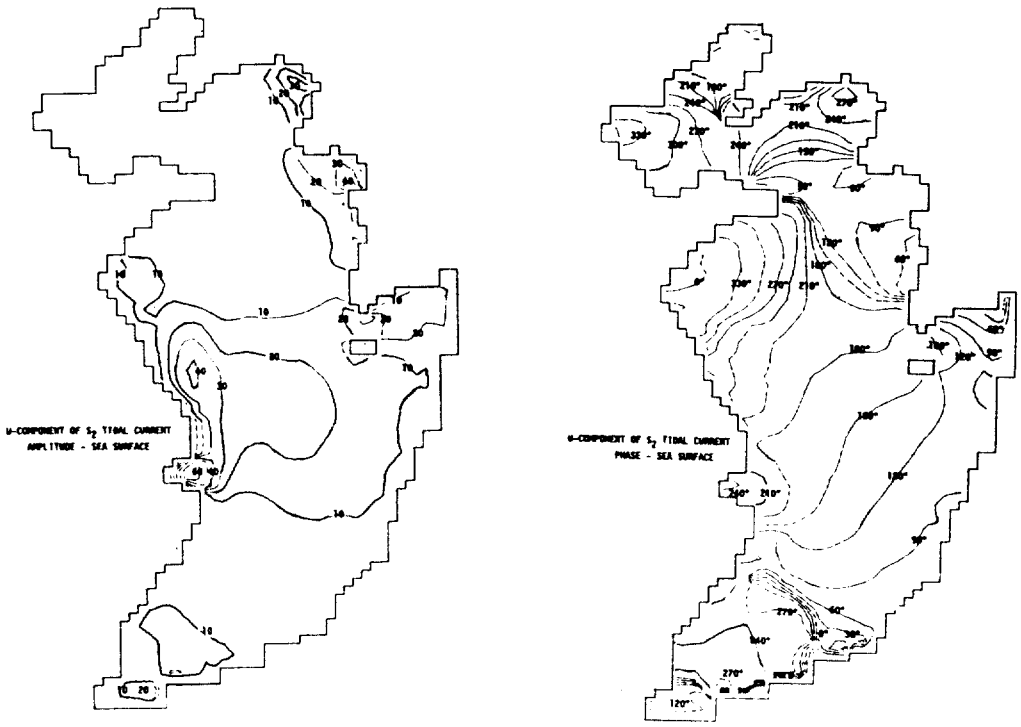
U-COMPONENT OF S_2 TIDAL CURRENT
AMPLITUDE - SEA SURFACE
U-COMPONENT OF S_2 TIDAL CURRENT
PHASE - SEA SURFACE

Fig. 3(a).

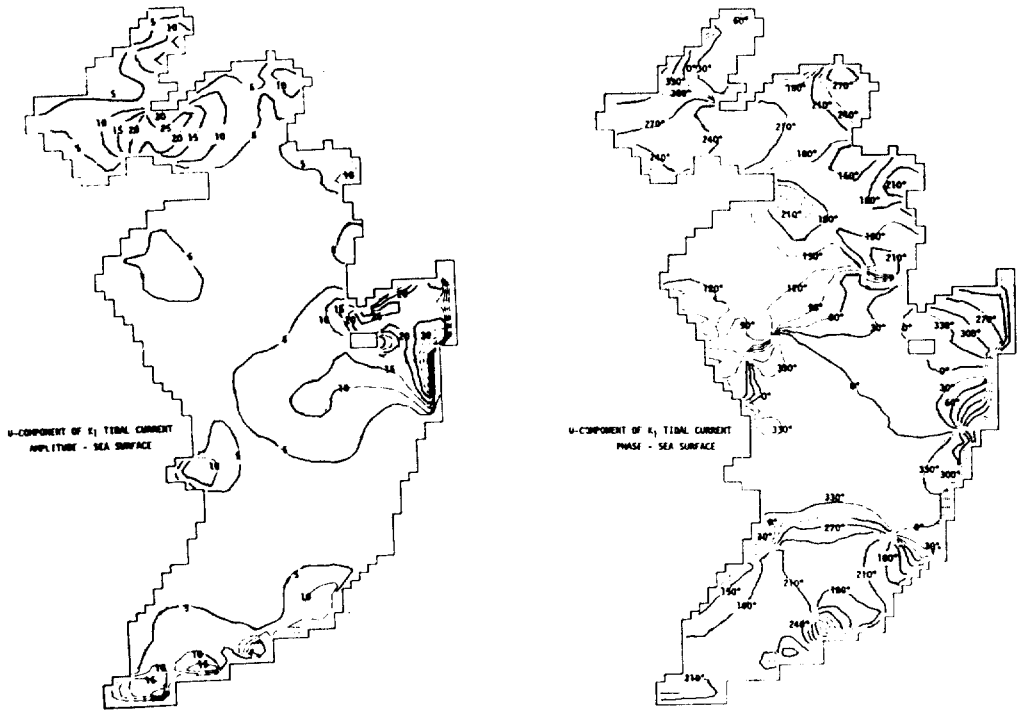
U-COMPONENT OF K_1 TIDAL CURRENT
AMPLITUDE - SEA SURFACE
U-COMPONENT OF K_1 TIDAL CURRENT
PHASE - SEA SURFACE

Fig. 3(b).

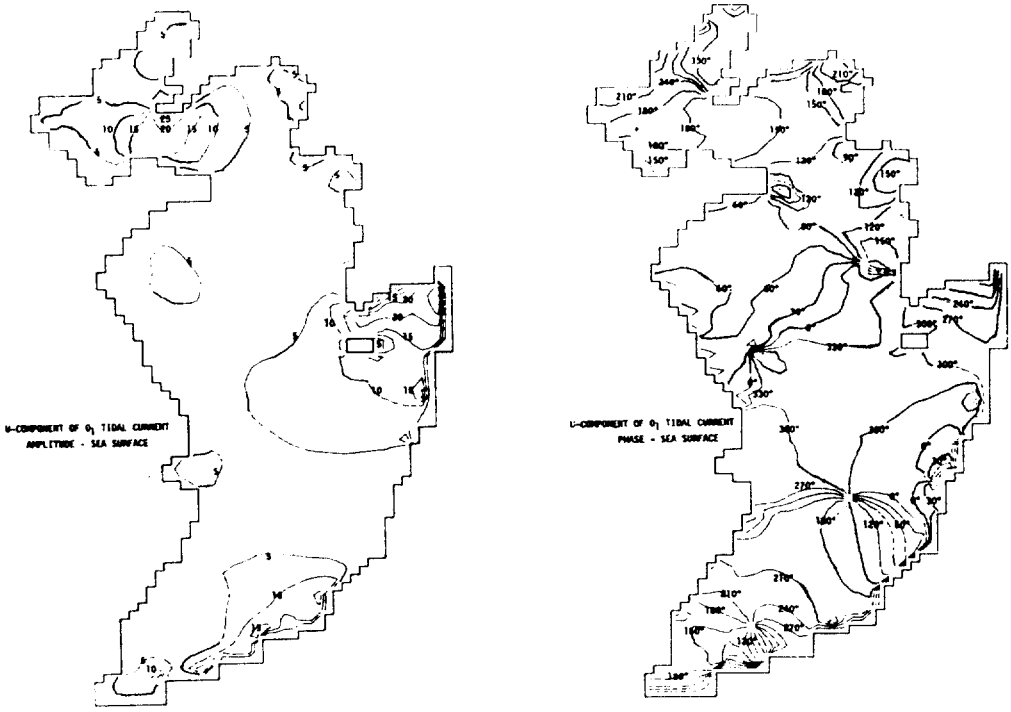

Fig. 3. (c).

Fig. 3. U-component of the S_2, K_1 and O_1 tidal currents at the sea surface.

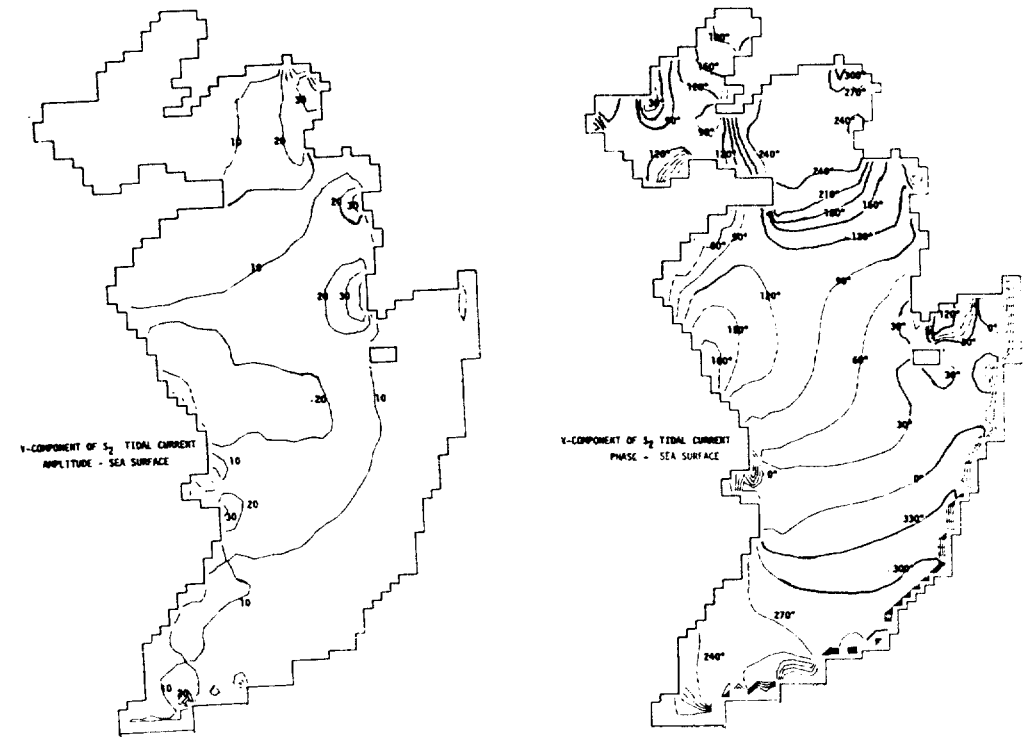

Fig. 4(a).

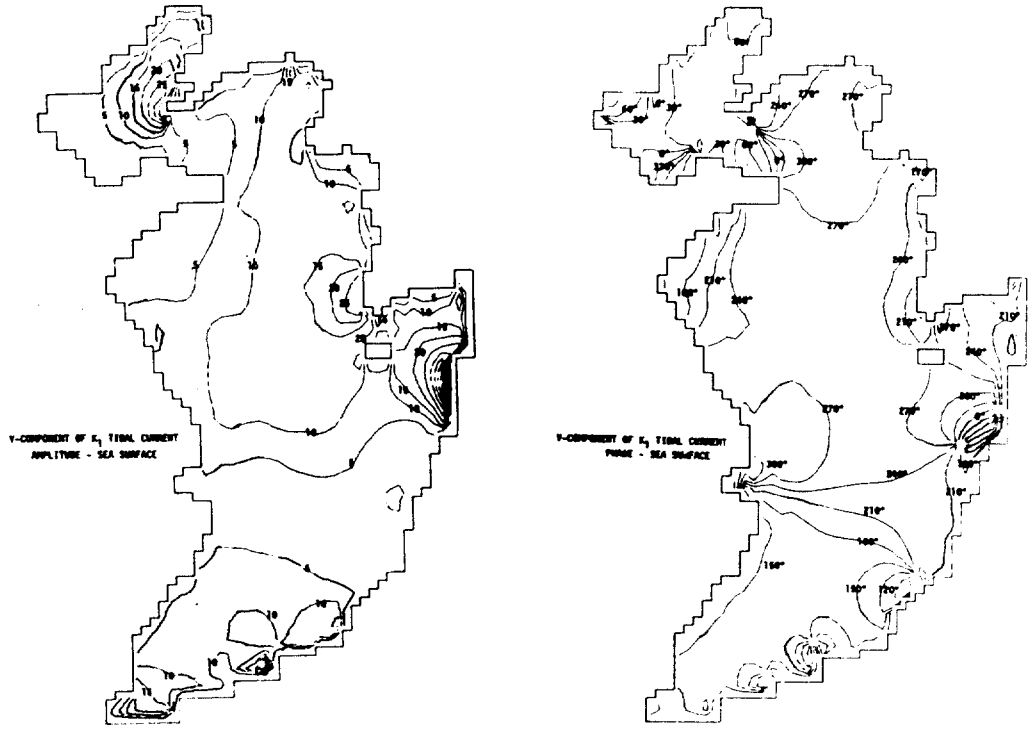

Fig. 4(b).

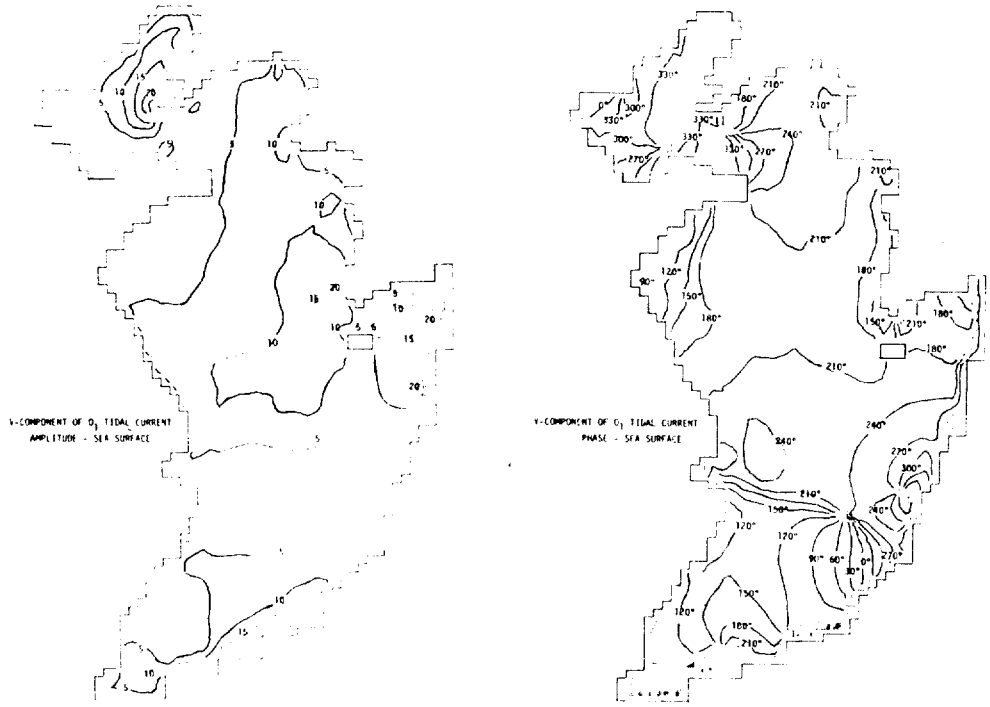

Fig. 4(c).

Fig. 4. V-component of the S_2, K_1 and O_1 tidal currents at the sea surface.

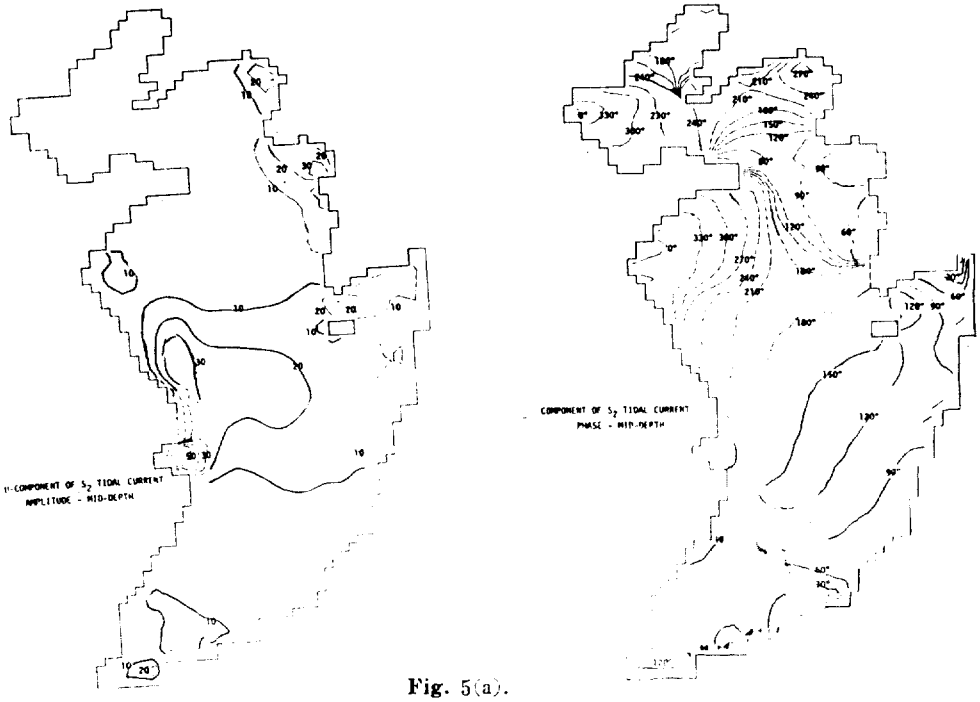
M-COMPONENT OF S_2 TIDAL CURRENT
AMPLITUDE - MID-DEPTH
COMPONENT OF S_2 TIDAL CURRENT
PHASE - MID-DEPTH

Fig. 5(a).

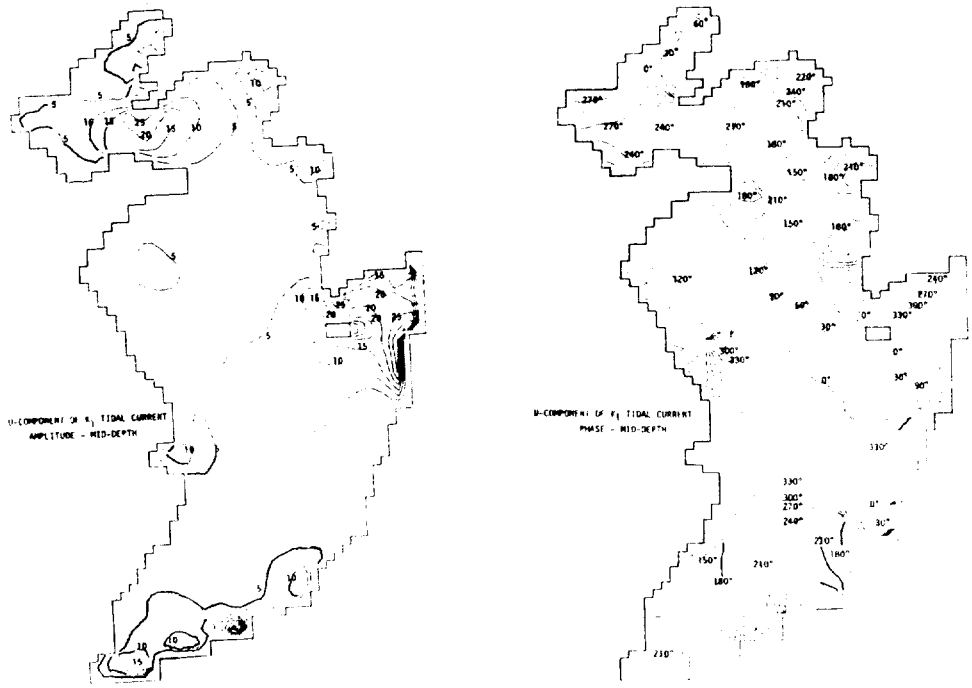
M-COMPONENT OF K_1 TIDAL CURRENT
AMPLITUDE - MID-DEPTH
M-COMPONENT OF K_1 TIDAL CURRENT
PHASE - MID-DEPTH

Fig. 5(b).

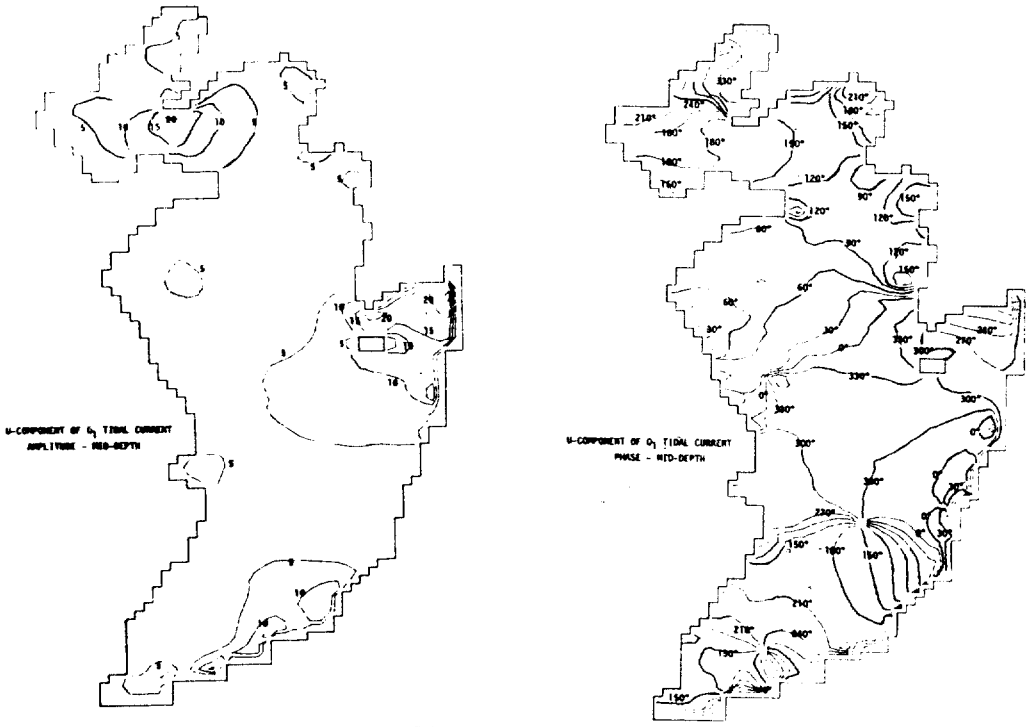

Fig. 5(c).

Fig. 5. U-component of the S_2, K_1 and O_1 tidal currents at the mid-depth.

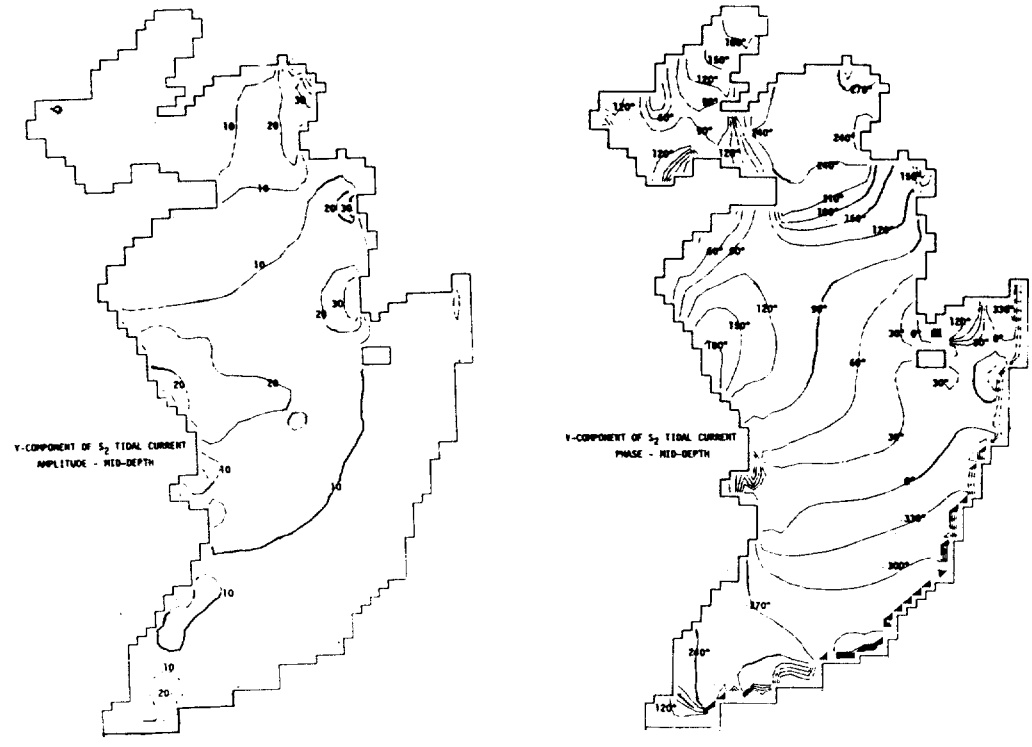

Fig. 6(a).

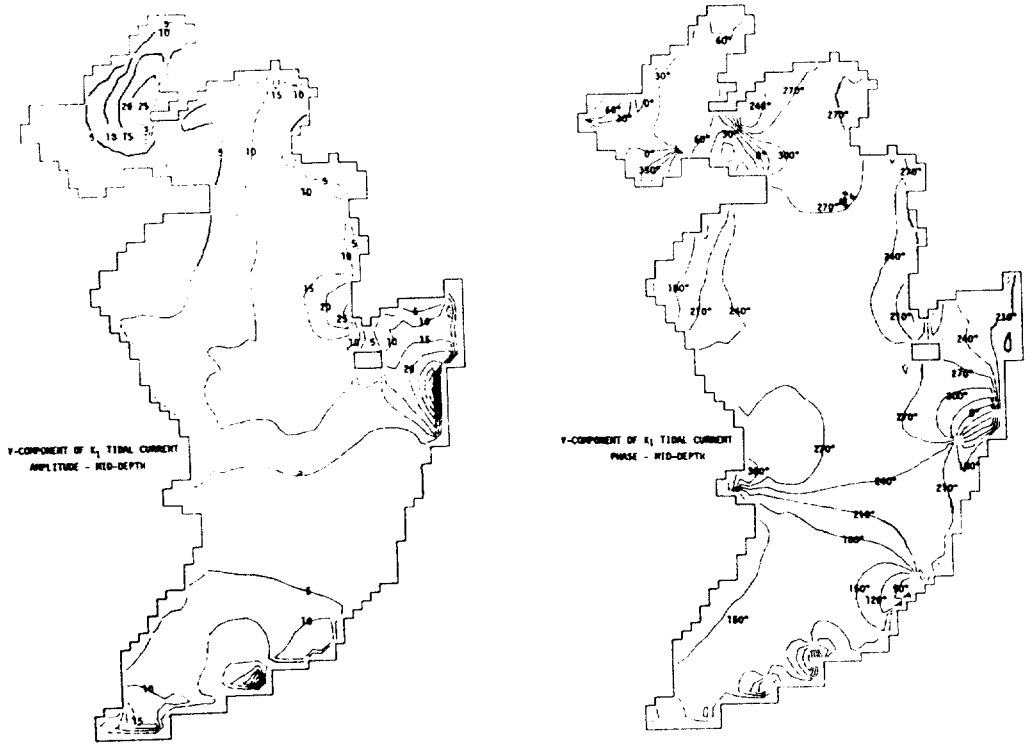

Fig. 6(b).

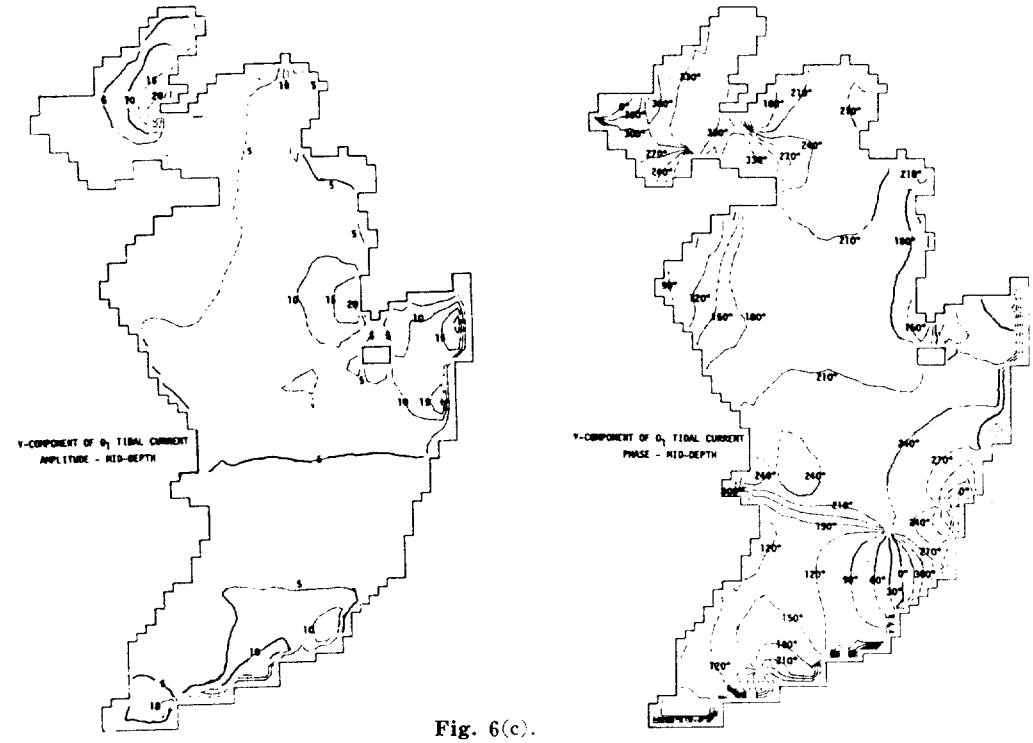

Fig. 6(c).

Fig. 6. V-component of the S_2, K_1 and O_1 tidal currents at the mid-depth.

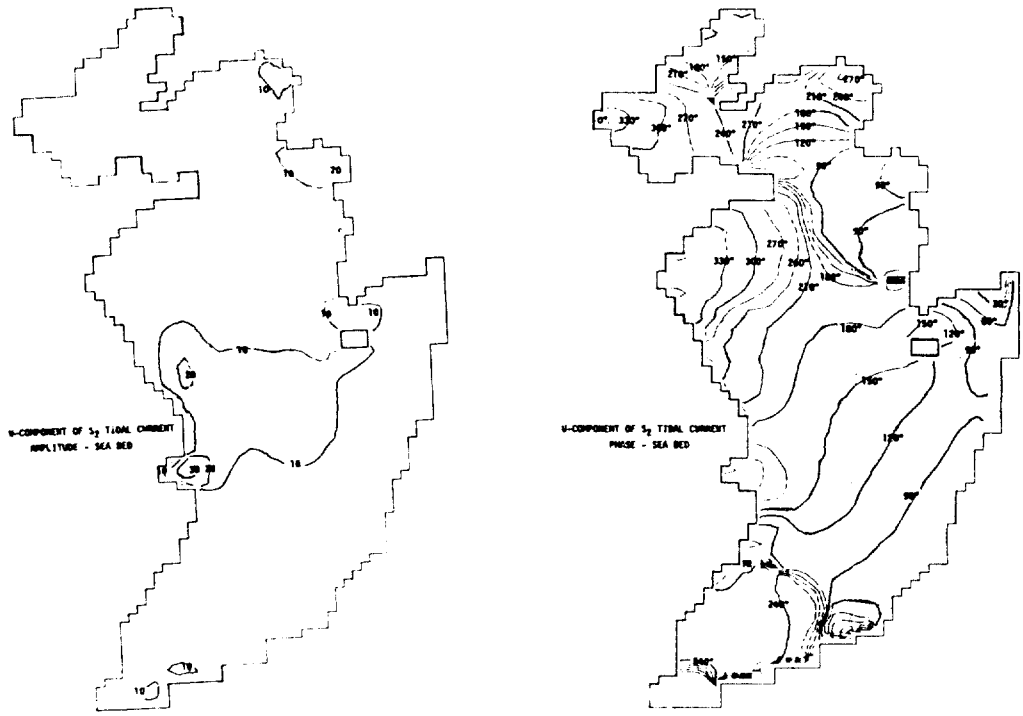
U-COMPONENT OF S_2 TIDAL CURRENT
AMPLITUDE - SEA BED
U-COMPONENT OF S_2 TIDAL CURRENT
PHASE - SEA BED

Fig. 7(a).

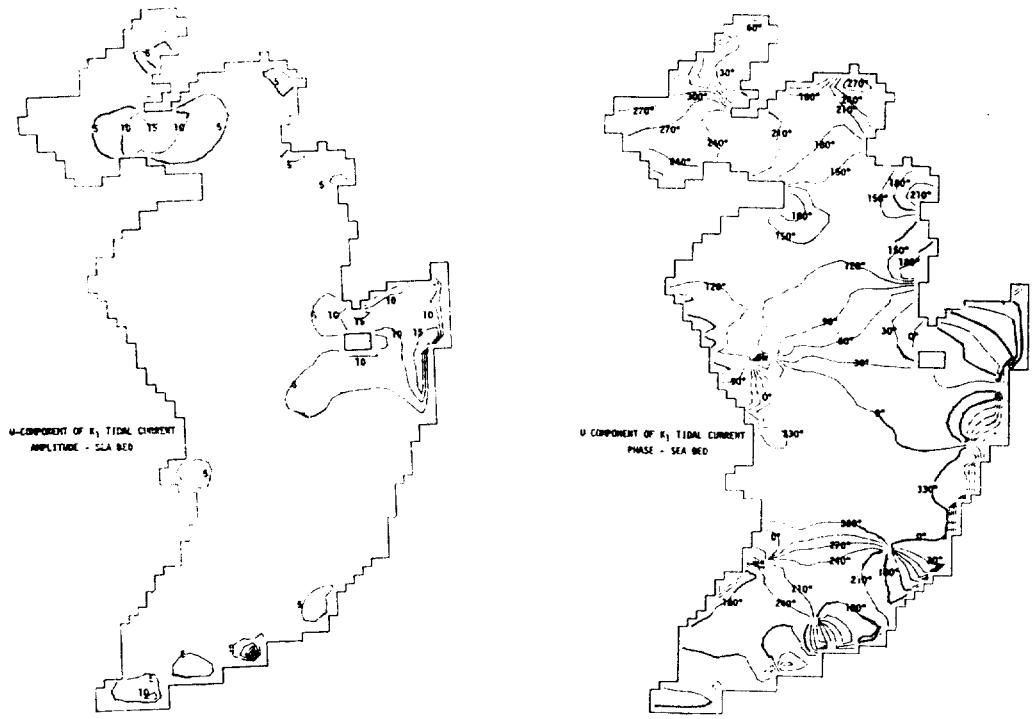
U-COMPONENT OF K_1 TIDAL CURRENT
AMPLITUDE - SEA BED
U COMPONENT OF K_1 TIDAL CURRENT
PHASE - SEA BED

Fig. 7(b).

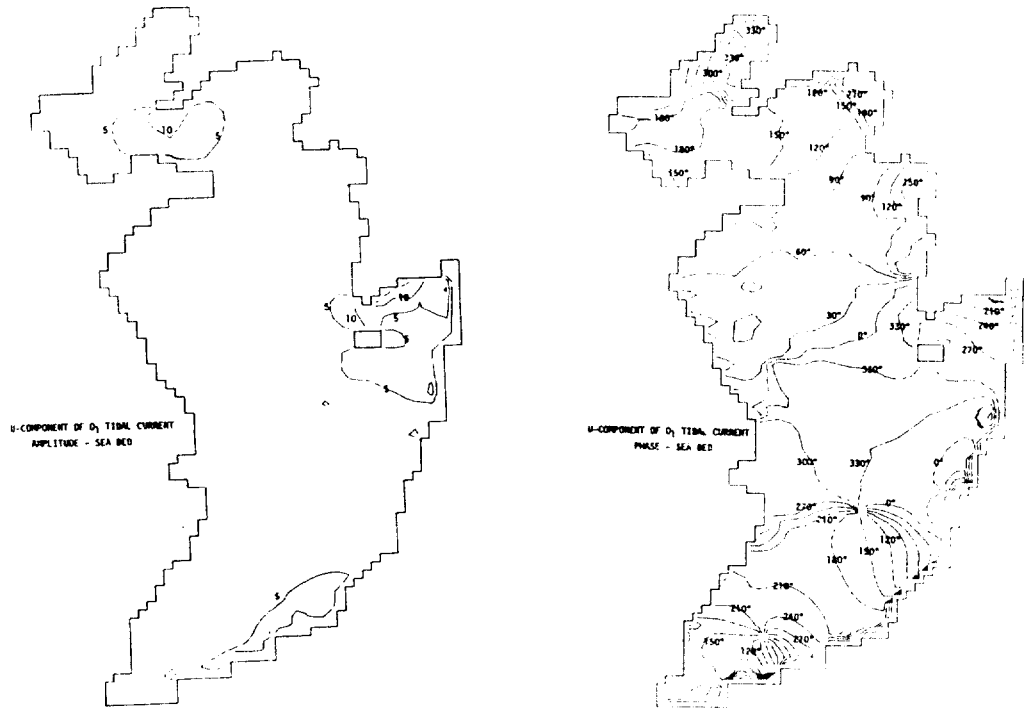

Fig. 7(c).

Fig. 7. U-component of the S_2, K_1 and O_1 tidal currents at the sea bed.

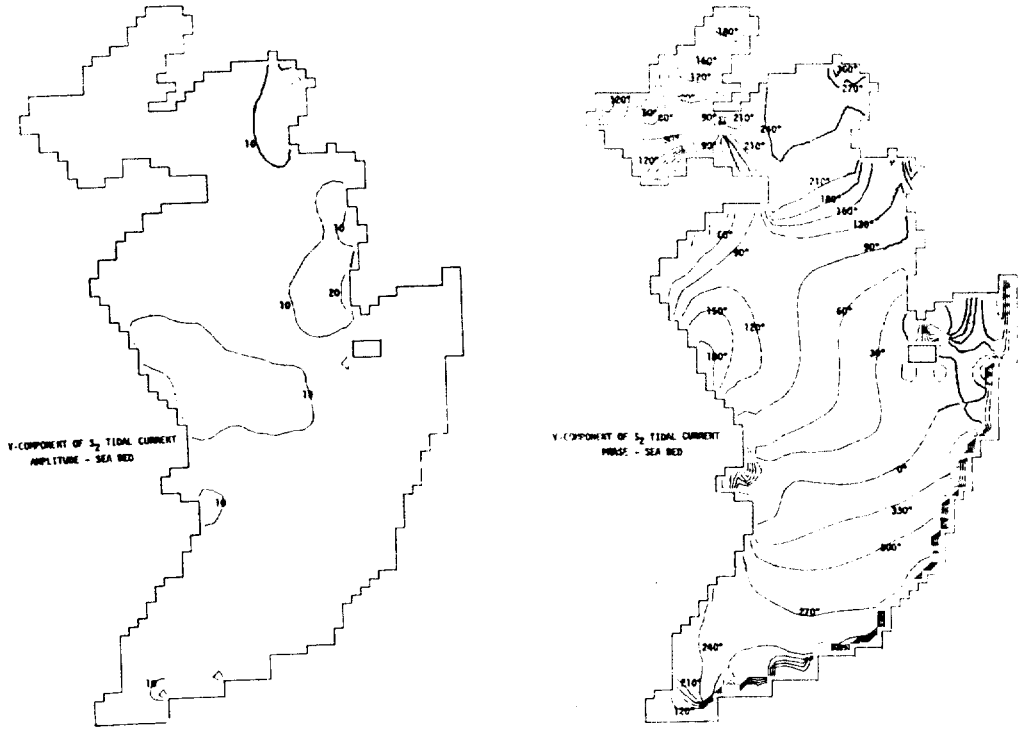

Fig. 8(a).

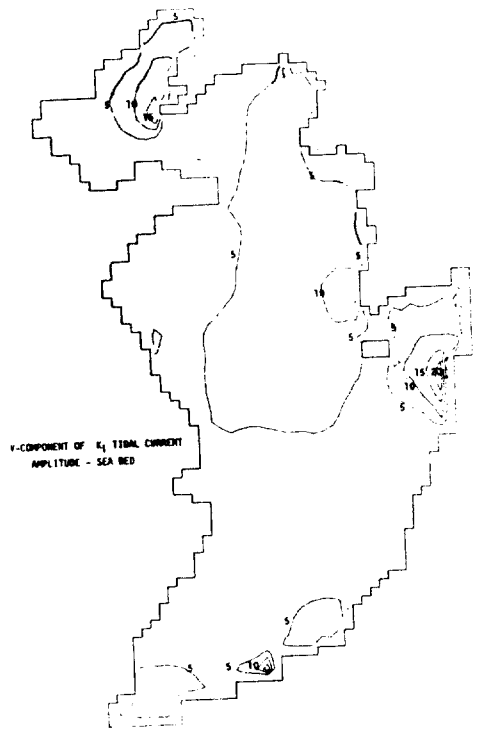

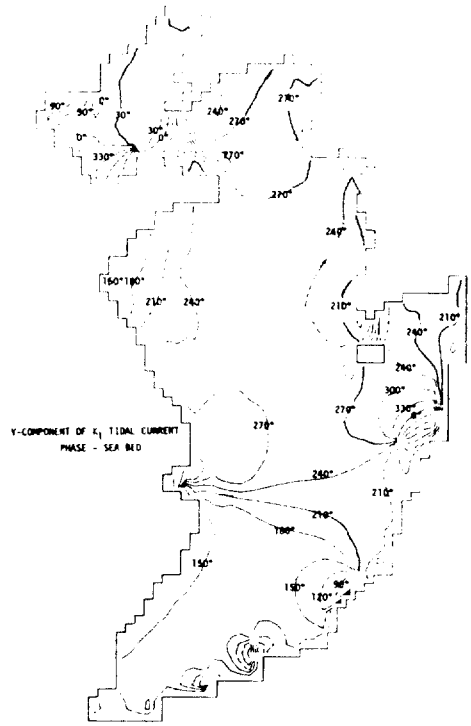

Fig. 8(b).

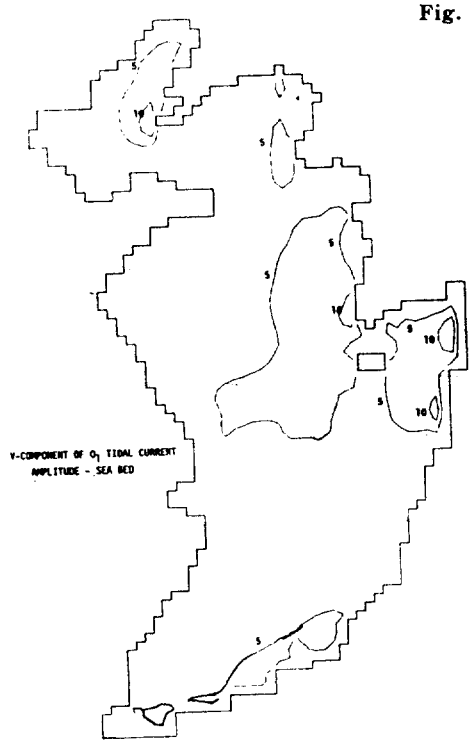

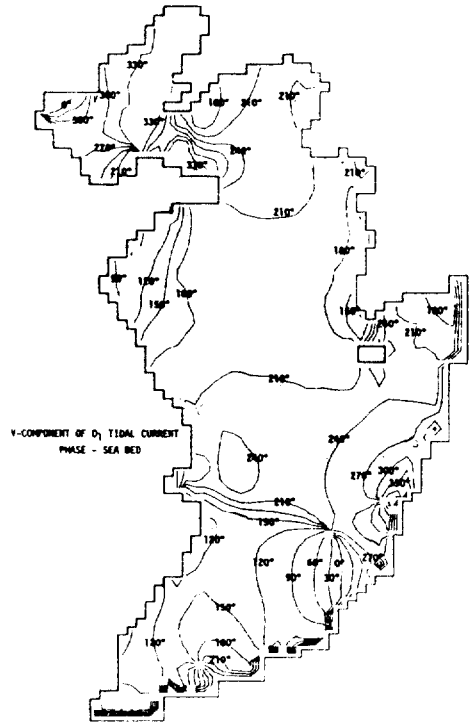

Fig. 8(c).

Fig. 8. V-component of the S_2, K_1 and O_1 tidal currents at the sea bed.

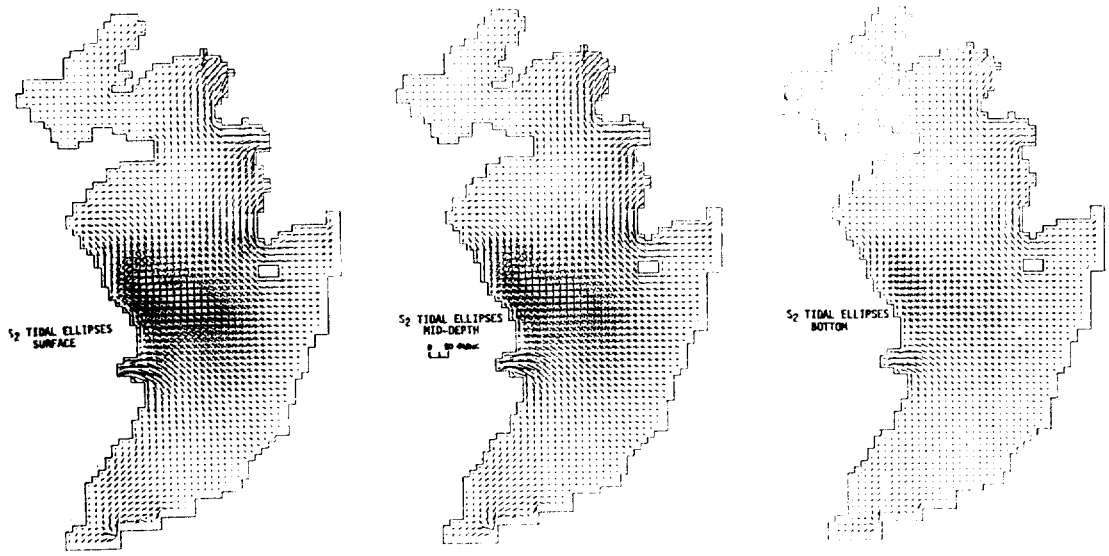

Fig. 9. Computed principal axes of the S_2 tidal ellipses.

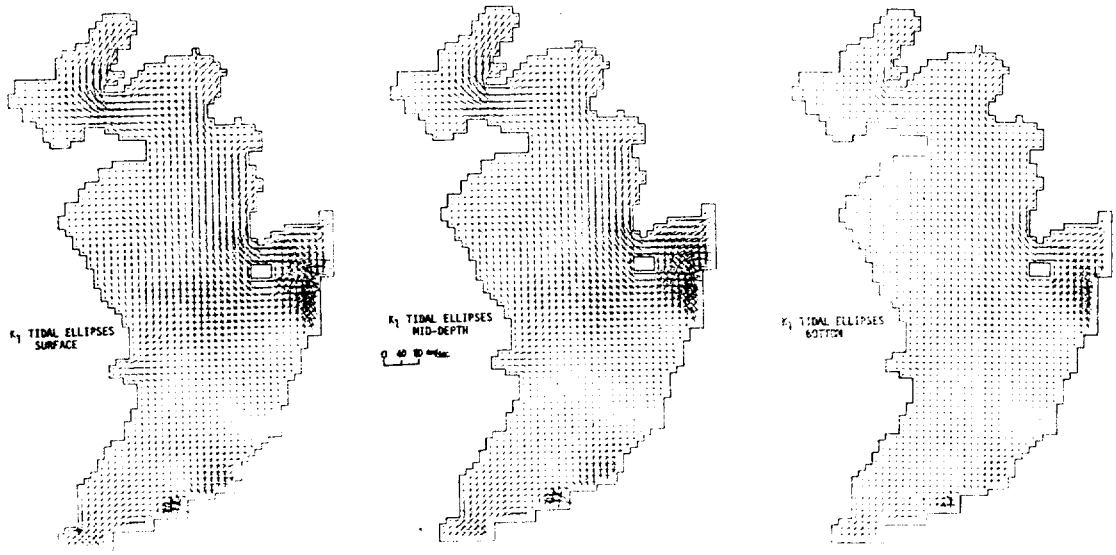

Fig. 10. Computed principal axes of the K_1 tidal ellipses.

These ellipses give an overall impression of the magnitude and direction of the S_2, K_1 and O_1 tidal currents distribution representing the maximum and minimum velocities as major and minor axes respectively.

It is worth noting from the S_2 tidal ellipses chart that rotating current patterns in the lower part of the East China Sea are in good agreement with speculation of Ogura (1933). In near coastal areas, elongated major axes indicates the current is rectilinear. Highest surface S_2 tidal currents computed are of the order of 50cm/sec. in Inchon Bay, Hangzhou Bay, in the estuary of Yalu (Seonhan Bay) and Changjiang Rivers. S_2 tidal currents generally rotate counterclockwise in the Gulfs of Liautung and Pohai, Seohan Bay, the west coast of Korea, southern part of hantung Peninsula,

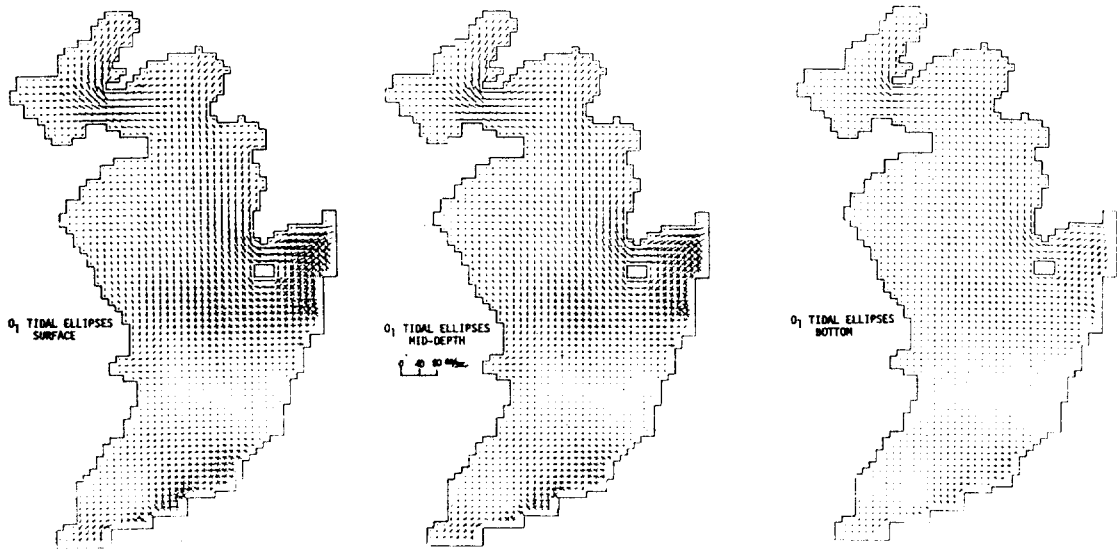

Fig. 11. Computed principal axes of the O_1 tidal ellipses.

south coastal waters of Korea, Hangzhou Bay and the northern sea area of Taiwan. S_2 tidal currents rotate clockwise in the Pohai Strait, in the lower part of the Yellow Sea and over the East China Sea.

It is seen from diurnal tidal ellipses charts that highest surface currents computed are of the order of 25~40cm/sec. for K_1 tidal current and 20~30 cm/sec. for O_1 tidal current in the Pohai Strait, Offshore of southwestern tip of Korean Peninsula and the shelf edge region off the Kyushu Islands. Eoth K_1 and O_1 tidal currents rotate counterclockwise in the Yellow Sea, the upper region of line connecting the estuary of Changjiang River and southwestern tip of Korean Peninsula except the northern part of the Shantung Peninsula and part of the Seohan Bay. Both K_1 and O_1 tidal currents rotate clockwise in the lower part of the above-mentioned line covering the whole East China Sea shelf.

CONCLUDING REMARKS

A three-dimensional tidal model for the Yellow Sea and the East China Sea has been formulated to compute a continuous representation of the current from the sea surface to the sea bed. The three-dimensional model was applied to the Yellow Sea and the East China Sea continental shelf, and the results were used to provide maps of the major tidal current constants at three depths. The general agreement between the current observations and computed currents is presented. Further numerical experiments for model improvement employing varying vertical eddy viscosity and variation of bottom friction coefficients are being performed in conjunction with extensive field measurement programme.

ACKNOWLEDGEMENTS

Modelling work described here was initiated during my visit to Bidston Observatory. The author is indebted to scientists in the dynamic modelling group of Bidston Observatory. Funding for this work was provided by Korea Research Foundation. Computational assistance from KAIST Compter Center Center is also acknowledged and the model has run about five c.p.u. hours on IBM 3025.

REFERENCES

Choi, B.H., 1980. A tidal model of the Yellow Sea and the Eastern China Sea. Korea Ocean Research and Development Institute (KORDI), rep. 80-02, 72pp.

Choi, B.H., 1984. A three-dimensional model of the East China Sea. pp. 209-224. in Ocean Hydrodynamics of the Japan and East China Seas (ed. T. Ichiye), Amsterdam, Elsevier.

Davies, A.M., 1980. On formulating a three-dimensional sea model with an arbitrary variation of vertical eddy viscosity. Computer Methods in Applied Mechanics and Engineering, 22:187-211.

Heaps, N.S., 1972. On the numerical solution of the thee-dimensional hydrodynamical equations for tides and storm surges. Mem. Soc. Roy. Sci. Liège, 2: 143-180.

Larsen, L.H. and Cannon, G.A., 1983. Tides in the East China Sea. Paper presented to Symposium on Sedimentation on the Continental Shelf, April 1983, Hangzhou, China.

Ogura, S., 1933. The tides in the seas adjacent to Japan. Bulletin of Hydrographic department, Imperial Japanese Navy, 7, 189pp.